J Electr Eng Technol.2018; 13(5): 1927-1934
http://doi.org/10.5370/JEET.2018.13.5.1927

ISSN(Print) 1975-0102
ISSN(Online) 2093-7423

# Battery State Estimation Algorithm for High-Capacity Lithium Secondary Battery for EVs Considering Temperature Change Characteristics

**Jinho Park*, Byoungkuk Lee*, Do-Yang Jung** and Dong-Hee Kim†**

**Abstract** – In this paper, we studied the state of charge (SOC) estimation algorithm of a high-capacity lithium secondary battery for electric vehicles (EVs) considering temperature characteristics. Nonlinear characteristics of high-capacity lithium secondary batteries are represented by differential equations in the mathematical form and expressed by the state space equation through battery modeling to extract the characteristic parameters of the lithium secondary battery. Charging and discharging equipment were used to perform characteristic tests for the extraction of parameters of lithium secondary batteries at various temperatures. An extended Kalman filter (EKF) algorithm, a state observer, was used to estimate the state of the battery. The battery capacity and internal resistance of the high-capacity lithium secondary battery were investigated through battery modeling. The proposed modeling was applied to the battery pack for EVs to estimate the state of the battery. We confirmed the feasibility of the proposed study by comparing the estimated SOC values and the SOC values from the experiment. The proposed method using the EKF is expected to be highly applicable in estimating the state of the high-capacity rechargeable lithium battery pack for electric vehicles.

**Keywords**: Battery modeling, Electric vehicles, Lithium-ion battery, State of charge, Extended Kalman filter, State space equation.

## 1. Introduction

Countries worldwide are experiencing adverse effects such as depletion of fossil fuel resources, intensification of atmospheric pollution, and greenhouse effects caused by $CO_2$ due to rapid industrialization. Therefore, awareness regarding environment protection is getting stronger, and environmental regulations have been strengthened to protect the world environment. Major developed countries are obliged to label their energy efficiency to save energy and to strive for carbon emission reduction, to mitigate the yearly increase in greenhouse gas. Particularly, the interest in environmentally friendly cars and the efforts to expand the market are increasing to reduce carbon emissions from the internal combustion engine that emits exhaust gases [1].

Korea has also been actively promoting eco-friendly cars such as electric cars, as government support policies and strong investments from industry have recently occurred. As the market becomes more active, the interest in electric vehicles (EVs) with high power and high-capacity batteries is increasing. Since the batteries used in electric vehicles require high capacity and high power, rechargeable lithium batteries with excellent performance are being used. Further, the battery pack applied to all electric vehicles is equipped with a battery management system (BMS), which detects and estimates the state of the battery in real time. The battery status information acquired by the BMS is provided to the vehicle for efficient driving and control [2-5].

In this paper, we propose a battery state estimation method to efficiently control the high-capacity lithium secondary battery for EVs, an environmentally friendly automobile. Since the electric vehicle battery requires a large change in instantaneous power, a technology capable of controlling the voltage and current in real time is required. Therefore, an algorithm that can accurately estimate the battery state in real time is needed. Status

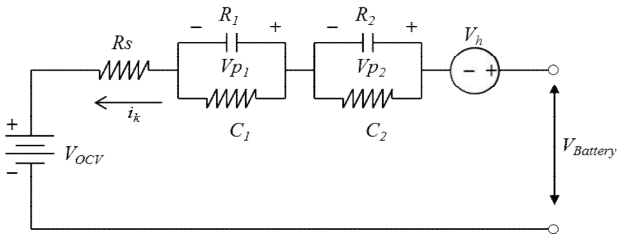


**Fig. 1.** Battery model with RC circuit

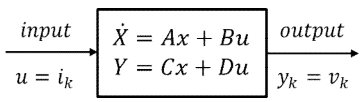


**Fig. 2.** State space equation for battery model

† Corresponding Author: Department of Electrical Engineering, Chonnam National University, Korea. (kimdonghee@jnu.ac.kr)
* Department of Electrical and Computer Engineering, Sungkyunkwan University, Korea. (pjh6001@gmail.com, bkleeskku@skku.edu)
** PNE SYSTEMS Corporation, Korea. (jungdy@pnesys.co.kr)
Received: January 11, 2018; Accepted: April 3, 2018

information such as SOC and state of health (SOH) of the battery cannot be simply measured or calculated, and they should be precisely estimated through the investigation and analysis of battery parameters. Therefore, the battery state estimation algorithm requires a mathematical differential equation that reflects a multidimensional nonlinear system since the charging and discharging characteristics of a lithium secondary battery are not linear.

In this paper, battery modeling is performed by expressing the temperature characteristic and internal resistance of the lithium secondary battery by the state space equation, and the SOC estimation technique of the battery is studied by applying the EKF as a state observer. To validate this study, we applied a driving profile to simulate a real vehicle to determine the state of a lithium secondary battery pack for an electric vehicle.

## 2. Li-ion Battery Modeling and Parameters Extraction

### 2.1 Battery modeling using state space equation

The lithium secondary battery is a nonlinear system of which its charging and discharging characteristics are different. To estimate the SOC of the battery, an electric circuit model is utilized and the governing equations of the battery model is expressed as state space equations of the differential equations.

The electric circuit of the battery model should be configured as an RC ladder as a continuous nonlinear model using internal parameters such as the nominal capacity of the battery, internal resistance, conduction resistance, and diffusion resistance.

The terminal voltage of the lithium secondary battery model is expressed by (1).

$$V_{bat} = V_{ocv} + Ri_k + V_{p1} + V_{p2} + V_h \tag{1}$$

To estimate the state of the lithium secondary battery, the state space equation and state variables were used. In this paper, battery modeling is performed using the enhanced self-correcting (ESC) model, which can demonstrate the nonlinear characteristics of the lithium secondary battery. The state of the selected lithium secondary battery model is estimated based on the input current and the output voltage. The ESC model represented by the state space equation is given by (2) and (3), (4). [3].

$$\begin{bmatrix} f_{k+1} \\ h_{k+1} \\ Z_{k+1} \end{bmatrix} = \begin{bmatrix} diag(\alpha) & 0 & 0 \\ 0 & F(i_k) & 0 \\ 0 & 0 & 1 \end{bmatrix} \begin{bmatrix} f_k \\ h_k \\ Z_k \end{bmatrix} + \begin{bmatrix} B_f & 0 \\ 0 & 1-F(i_k) \\ -\dfrac{\Delta t}{C_n} & 0 \end{bmatrix} \begin{bmatrix} i_k \\ \mathrm{sgn}(i_k) \end{bmatrix} \tag{2}$$

$$y_k = OCV(Z_k) + Ri_k + Mh_k + filt(i_k) \tag{3}$$

where, $F(i_k)$ is defined by

$$F(i_k) = \exp\left( -\left| \frac{\gamma \cdot i_k \cdot \Delta t}{C_n} \right| \right) \tag{4}$$

Where, $y_k$ is the output voltage of the proposed modeling, which is represented by the open-circuit voltage (OCV) corresponding to the state variable SOC($Z_k$), the low-pass filter *filt* ($i_k$) that receives the current generated by the battery charge/discharge, the internal resistance of the battery ($R$), the input current ($i_k$), the hysteresis ($h_k$) that appears differently during polarization and discharge because of the difference in electrolyte concentration, the battery's nominal capacity ($C_n$), the estimate of the battery's internal resistance has different values for charge($R^+$) and discharge ($R^-$) conditions. the vector representing the filter poles ($\alpha_1$), the polarization ($M$) according to hysteresis, the hysteresis rate constant ($\gamma$) and the battery modeling parameter $\theta$ that can be expressed as $\theta = [\alpha_1, g_1, \gamma, C_n, R^+, R^-, M]$.

In this equation, the function of the filter $filt(i_k)$ leads the output voltage $y_k$ to converge to $OCV$ after a resting period, and the output $y_k$ converges to OCV + $h_k$ + $Ri_k$ including the OCV when charging/discharging with a constant current. The linear filter is implemented by the state space equation, as shown in the following form (5).

$$\begin{aligned} f_{k+1} &= A_f f_k + B_f i_k \\ y_k^f &= G f_k \end{aligned} \tag{5}$$

where, $f_k$ is the filter state vector at a discrete time $k$, $i_k$ is the input vector, $y_k^f$ is the filter output vector, $A_f$ is the state-transition matrix of the filter, $B_f$ is the input matrix of the filter. $G$ is the output matrix of the filter.

### 2.2 Battery test for parameter extraction

The test for extracting the parameters used in the battery modeling was performed using the NMC (Lithium Nickel Manganese Cobalt Oxide)-type lithium secondary battery cell. The test was carried out using the unit cell of a 2-parallel and the module consisting of 2-parallel and 9-series as shown in Fig. 3. For the battery model of the selected lithium secondary battery, the reference temperature was selected as 25 °C, and then the battery characteristics was extracted at various temperatures using a temperature-controlled chamber.

The battery characteristics test for the parameter extraction was carried out using the driving profile of the fuel economy test mode of the vehicle. This profile has the advantage of simulating a dynamic situation rather than a constant current, therefore, the proposed battery modeling

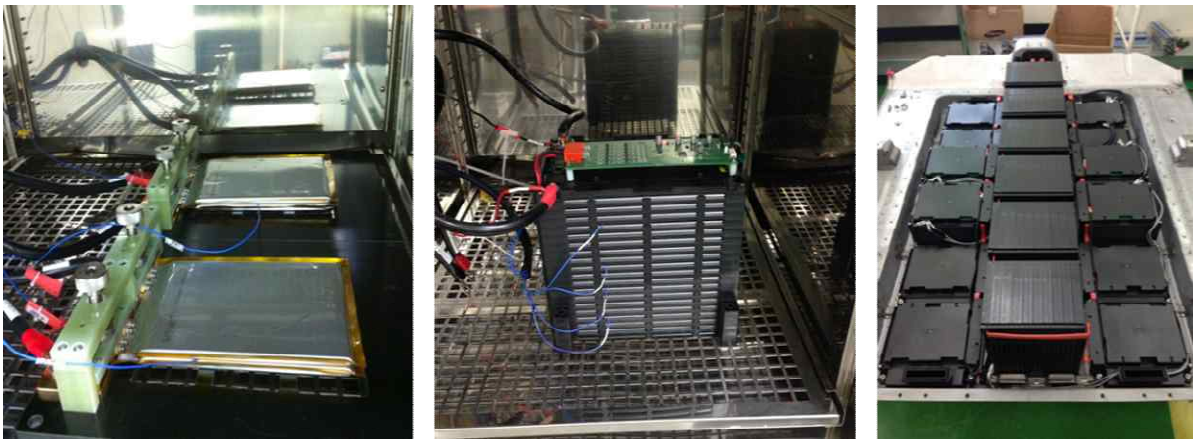

(a) 2P cell unit (b) 2P-9S module (c) 20 kWh pack

**Fig. 3.** Battery test for parameter extraction

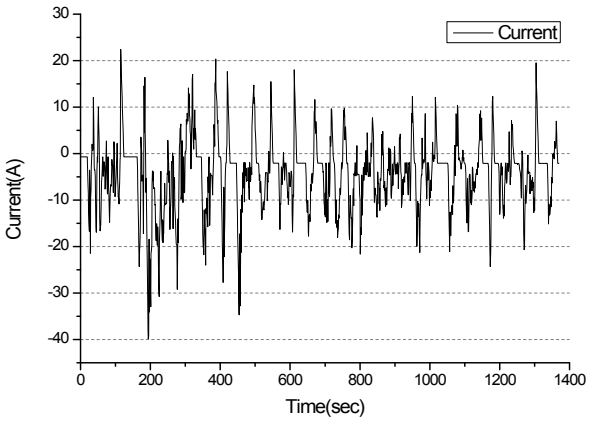


**Fig. 4.** UDDS Profile

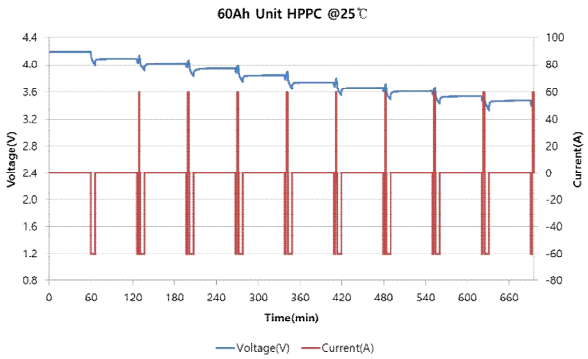


**Fig. 5.** HPPC test results of the battery cell with a 2-parallel connection.

**Table 1.** Battery parameters at various temperatures

| | -10°C | 0°C | 10°C | 25°C | 35°C | 45°C |
|---|---|---|---|---|---|---|
| $\alpha_1$ | 1.718 | 2.572 | 2.385 | 2.245 | 2.275 | 2.365 |
| $g_1$ | 0.977 | 0.326 | 0.263 | 0.153 | 0.144 | 0.112 |
| $\gamma$ | 5.449 | -0.48 | 2.504 | 0.0 | 6.47 | 0.588 |
| $C_n$ | 45.738 | 52.405 | 54.003 | 62.376 | 61.879 | 60.157 |
| $R^-$ | 0.014 | 0.008 | 0.003 | 0.002 | 0.002 | 0.002 |
| $R^+$ | 0.013 | 0.008 | 0.003 | 0.002 | 0.002 | 0.002 |
| $M$ | 0.067 | -0.003 | -0.033 | -0.122 | 0.029 | 0.098 |

can be evaluated at the system level.

After selecting the parameters through the unit cell (2P) test, the selected unit cell parameter information was applied to a module and a pack system to examine the feasibility and the error of the model.

The driving profile used in the test was an urban dynamometer driving schedule (UDDS) cycle, in which the cycle is 1372 seconds, and the charging and discharging tests were repeated using the charging and discharging equipment from 100% to 0% SOC of the cell. The driving profile used for the characteristic test is shown in Fig. 4.

The parameter extraction tests were performed at temperatures of -10 °C, 0 °C, 10 °C, 25 °C, 35 °C, and 45 °C.

The output information of the battery is stored every 1 second. The parameter extraction is carried out through the profile application test, and the combination of the parameters is searched to obtain the minimum error with respect to the input/output of 12,000 or more. Since the output characteristics of a lithium secondary battery have a continuity of a multidimensional nonlinear system, it cannot be perfectly solved mathematically. Therefore, the extracted parameters can be regarded as a partial set of parameters that cannot be defined as a whole parameter of the battery. This can be analyzed using linear filtering such as the least square method. Table 1 shows the battery parameters selected by testing at various temperatures.

After selecting the parameters of the battery model at various temperatures, the fitness of the internal resistance parameter was verified using the hybrid pulse power characterization (HPPC) output test method. Fig. 5 shows the changes in voltage and current at 25 °C. The charging resistance and discharging resistance at each temperature are shown in Table 2 and Fig. 6.

The average value of the internal resistance obtained through the HPPC test and the internal resistances selected through modeling showed similar values above 10 °C, and

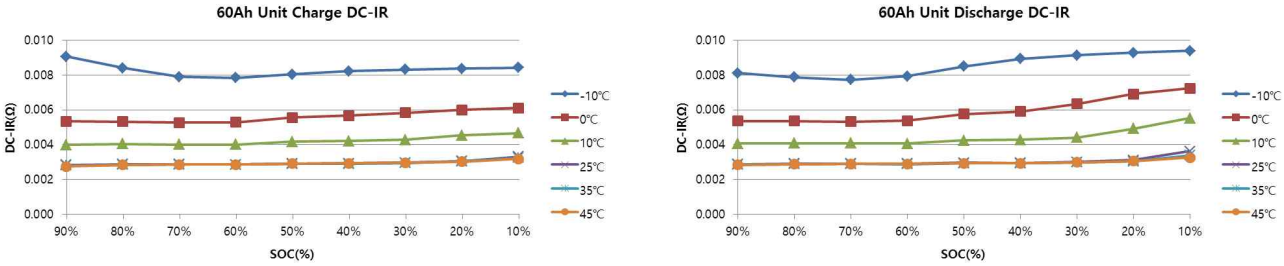


(a) DC-IR under charge (b) DC-IR under discharge

**Fig. 6.** 2P DC-IR test results of unit cell

**Table 2.** 2P DC-IR of unit cell

| Temp \ SOC | | 90% | 80% | 70% | 60% | 50% | 40% | 30% | 20% | 10% | Avg. |
|---|---|---|---|---|---|---|---|---|---|---|---|
| -10°C | $R^-(\Omega)$ | 8.1e-3 | 7.9e-3 | 7.7e-3 | 7.9e-3 | 8.5e-3 | 8.9e-3 | 9.1e-3 | 9.3e-3 | 9.4e-3 | 8.1e-3 |
| | $R^+(\Omega)$ | 9.1e-3 | 8.4e-3 | 7.9e-3 | 7.8e-3 | 8.0e-3 | 8.2e-3 | 8.3e-3 | 8.4e-3 | 8.4e-3 | 9.1e-3 |
| 0°C | $R^-(\Omega)$ | 5.4e-3 | 5.4e-3 | 5.3e-3 | 5.4e-3 | 5.8e-3 | 5.9e-3 | 6.3e-3 | 6.9e-3 | 7.2e-3 | 5.4e-3 |
| | $R^+(\Omega)$ | 5.3e-3 | 5.3e-3 | 5.3e-3 | 5.3e-3 | 5.6e-3 | 5.7e-3 | 5.8e-3 | 6.0e-3 | 6.1e-3 | 5.3e-3 |
| 10°C | $R^-(\Omega)$ | 4.1e-3 | 4.1e-3 | 4.1e-3 | 4.1e-3 | 4.2e-3 | 4.3e-3 | 4.4e-3 | 4.9e-3 | 5.5e-3 | 4.1e-3 |
| | $R^+(\Omega)$ | 4.0e-3 | 4.0e-3 | 4.0e-3 | 4.0e-3 | 4.2e-3 | 4.2e-3 | 4.3e-3 | 4.5e-3 | 4.7e-3 | 4.0e-3 |
| 25°C | $R^-(\Omega)$ | 2.9e-3 | 2.9e-3 | 2.9e-3 | 2.9e-3 | 3.0e-3 | 2.9e-3 | 3.0e-3 | 3.1e-3 | 3.6e-3 | 2.9e-3 |
| | $R^+(\Omega)$ | 2.8e-3 | 2.9e-3 | 2.9e-3 | 2.9e-3 | 2.9e-3 | 2.9e-3 | 3.0e-3 | 3.1e-3 | 3.3e-3 | 2.8e-3 |
| 35°C | $R^-(\Omega)$ | 2.9e-3 | 2.9e-3 | 2.9e-3 | 2.9e-3 | 2.9e-3 | 2.9e-3 | 3.0e-3 | 3.0e-3 | 3.4e-3 | 2.9e-3 |
| | $R^+(\Omega)$ | 2.8e-3 | 2.8e-3 | 2.9e-3 | 2.9e-3 | 2.9e-3 | 2.9e-3 | 3.0e-3 | 3.0e-3 | 3.3e-3 | 2.8e-3 |
| 45°C | $R^-(\Omega)$ | 2.8e-3 | 2.9e-3 | 2.9e-3 | 2.9e-3 | 2.9e-3 | 2.9e-3 | 3.0e-3 | 3.0e-3 | 3.3e-3 | 2.8e-3 |
| | $R^+(\Omega)$ | 2.8e-3 | 2.8e-3 | 2.9e-3 | 2.9e-3 | 2.9e-3 | 2.9e-3 | 3.0e-3 | 3.0e-3 | 3.2e-3 | 2.8e-3 |

the differences were found to be 3-6 mΩ. Therefore, the internal resistance measured by the HPPC method should be considered for optimizing the battery model parameters at low temperatures.

### 2.3 Parameter optimization according to temperature

The output power of the lithium secondary battery rapidly decreases in the low temperature range. This is caused by the diffusion reaction of the electrolyte constituting the lithium secondary battery, which shows a very sensitive response to the temperature change. The output power of the lithium secondary battery at low temperatures is dominated by the diffusion resistance component according to the temperature change in the electrolyte. The capacity, OCV, and the parameters of the proposed model show a large temperature dependency. Therefore, the model applied at room temperature shows different behaviors at low temperatures; hence, a battery model that can be applied for a wide range of temperatures is needed. Therefore, the parameters of the model obtained from the 25 °C test selected as the reference should be optimized to reflect the characteristics at low temperatures.

The parameters obtained through the characteristic tests performed at various temperature conditions are described by the following multidimensional equations, and the parameters according to the temperature are expressed as (6) together with the temperature $T$ [3-5].

**Table 3.** Polynomial coefficients for different parameters

| Parameter | Polynomial coefficients (third order) | | | |
|---|---|---|---|---|
| | $C_3$ | $C_2$ | $C_1$ | $C_0$ |
| $\alpha_1$ | $3.98\cdot10^{-5}$ | $-2.54\cdot10^{-3}$ | $3.35\cdot10^{-2}$ | 2.40 |
| $g_1$ | $-1.9\cdot10^{-5}$ | $-1.53\cdot10^{-3}$ | $-3.64\cdot10^{-2}$ | $4.14\cdot10^{-1}$ |
| $\gamma$ | $3.78\cdot10^{-4}$ | $2.21\cdot10^{-2}$ | $-2.13\cdot10^{-1}$ | $5.87\cdot10^{-1}$ |
| $C_n$ | $-1.59\cdot10^{-4}$ | $6.40\cdot10^{-4}$ | $4.98\cdot10^{-1}$ | 5.09·10 |
| $R^-$ | $-1.43\cdot10^{-7}$ | $1.52\cdot10^{-5}$ | $-5.14\cdot10^{-4}$ | $7.38\cdot10^{-3}$ |
| $R^+$ | $-1.08\cdot10^{-7}$ | $1.26\cdot10^{-5}$ | $-4.63\cdot10^{-4}$ | $7.23\cdot10^{-3}$ |
| $M$ | $2.71\cdot10^{-6}$ | $7.75\cdot10^{-5}$ | $-6.49\cdot10^{-3}$ | $-6.5\cdot10^{4}$ |

$$y(T) = C_3T^3 + C_2T^2 + C_1T^1 + C_0 \quad (6)$$

Table 3 and Fig. 7 show the polynomial coefficients that form the polynomial equation, which is expressed by the general formula according to the temperature.

### 2.4 Comparison of modeling results and measured results

Tests were conducted to validate the proposed model for the battery module by applying the parameter values obtained by the characteristic tests on the unit cells of the battery modules. Using a temperature-controlled chamber, it was tested analyzed based on the results obtained from various temperatures ranging from low to high temperatures.

Fig. 8 shows the result of the modeling by applying the cell parameters according to temperature. As shown in the graph, the voltage estimation RMS error according to each

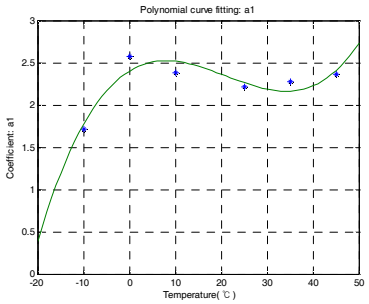


(a) $\alpha_1$

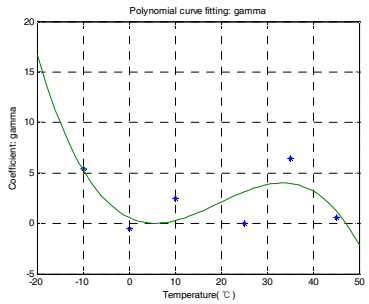


(b) $\gamma$

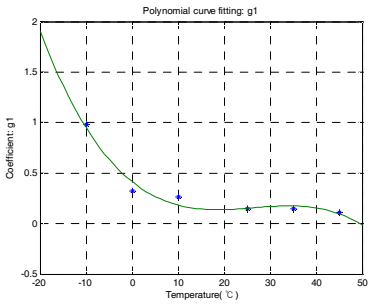


(c) $g_1$

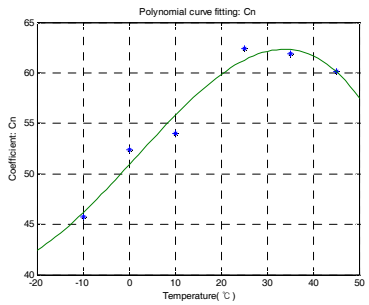


(d) $C_n$

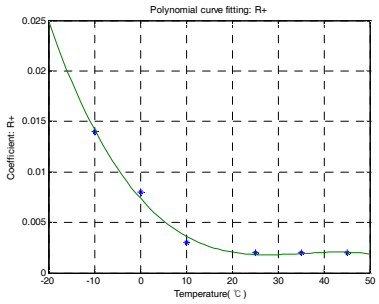


(e) $R^+$

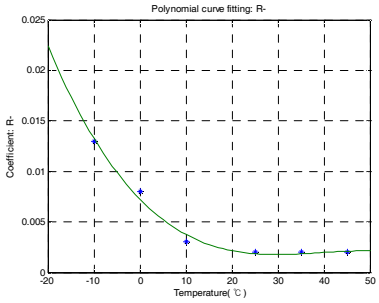


(f) $R^-$

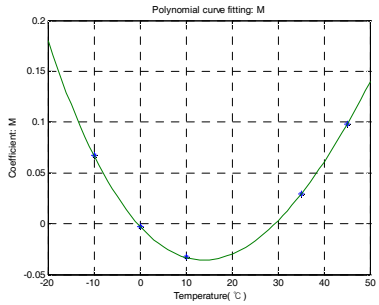


(g) $M$

**Fig. 7.** Parameter coefficients at various temperatures

**Table 4.** RMSE at various temperatures

| Temperature[°C] | -10 | 0 | 10 | 25 | 35 | 45 |
|---|---|---|---|---|---|---|
| Error Cost [V] | 0.128 | 0.087 | 0.078 | 0.026 | 0.023 | 0.023 |

temperature modeling was larger at low temperatures than it was at room temperature or high temperatures. The RMS error increasing at low temperatures can be attributed to the internal resistance at low temperatures, which differs significantly at room temperature. Therefore, since the internal resistance of the battery has a nonlinear characteristic, the error becomes large when the linear output equation is applied.

Table 4 and Fig. 8 show the difference between the test values at various temperatures and the estimated values from the battery modeling. The root mean squared error (RMSE) is shown in (7).

$$E = y - \hat{y} = \sqrt{\frac{E \times E'}{n}} \tag{7}$$

## 3. SOC Estimation and Verification using EKF

### 3.1 SOC estimation using EKF

To estimate the SOC of a lithium secondary battery, it is impossible to directly measure the SOC; therefore, it is necessary to estimate the SOC by an indirect method. In the estimation, the current integration method by current accumulation and the cell impedance measurement method

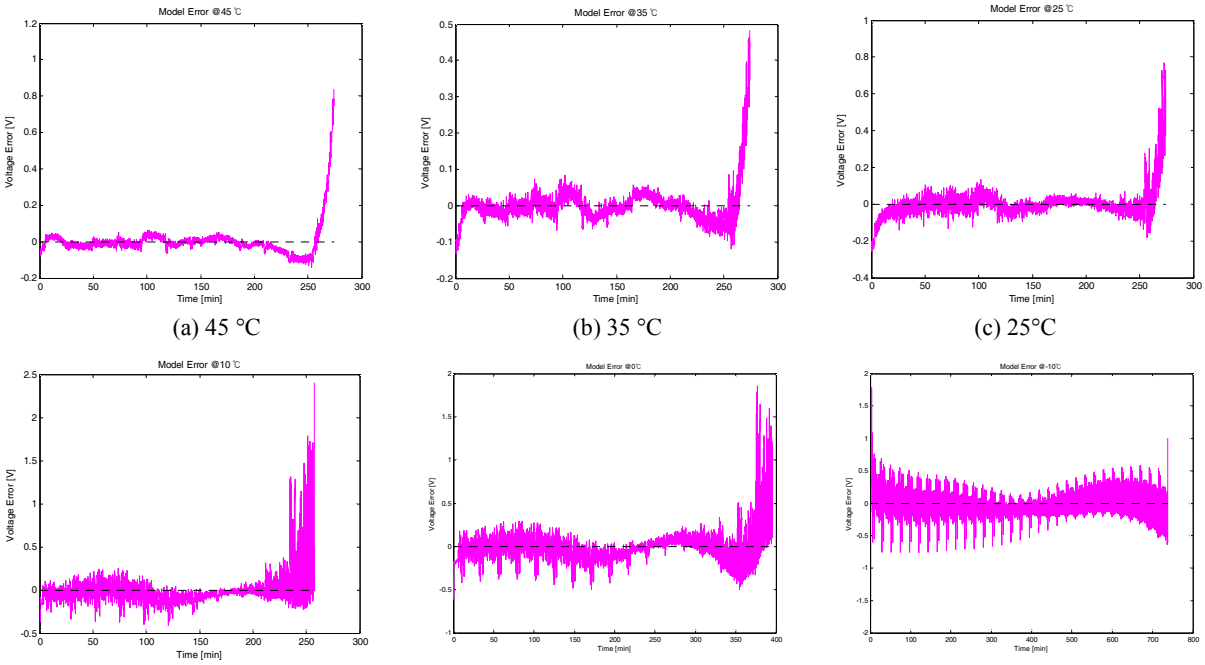


(a) 45 °C (b) 35 °C (c) 25°C

(d) 10°C (e) 0°C (f) -10°C

**Fig. 8.** Voltage estimation error results at various temperatures

**Fig. 9.** Battery pack of electric vehicle

utilizing an impedance, which is a resistance component of a battery cell are widely used. In this paper, we present a mathematical equation of state through battery modeling and then use the state observer to estimate the remaining capacity.

First, the state parameter of the battery is selected. Based on this value, the state variable of the SOC is obtained through the input current and the output voltage. The system consists of a state variable through the input and output, which can be measured. The Kalman filter (KF) used as the state observer is a filter used to predict the variables and can be predicted mathematically by minimizing the state error of the linear system. However, since the parameters of the battery are nonlinear, it is difficult to obtain satisfactory accuracy when simply applying the KF. Therefore, to apply the nonlinear system of the lithium secondary battery, the variable is estimated using an EKF. When the EKF is applied, it is possible to predict the SOC of the battery at 20%-90% of the SOC available area, and the accuracy of the SOC estimation is less than 5%. The EKF estimates the state $x$, which is SOC of the battery by the EKF, of the battery using the measurement voltage $y$ value, and minimizes the mean square error of the state estimation observation value $\hat{x}$. This is expressed by (8).

$$E[|x-\hat{x}||^2] = \sum_{i=1}^{n} E(x-\hat{x})^2 \tag{8}$$

The EKF equation, which is a nonlinear system, is defined as follows:

$$\begin{aligned} x(k+1) &= f(x(k),u(k)) + w_k \\ y(k) &= g(x(k),u(k)) + v_k \end{aligned} \tag{9}$$

$$\begin{aligned} \hat{A}(k) &= \left.\frac{\partial f(x(k),u(k))}{\partial x_k}\right|_{x_k=\hat{x}_k^+} \\ \hat{C}(k) &= \left.\frac{\partial g(x(k),u(k))}{\partial x_k}\right|_{x_k=\hat{x}_k^-}, \end{aligned} \tag{10}$$

where $w_k$ and $v_k$ represent the white Gaussian noise with an average of zero. At each time step, $f(x(k),u(k))$ and $g(x(k),u(k))$ are the Taylor-series expansions, and the EKF loop is as follows: [6-9]

1) Initial value selection: ($k = 0$)

$$\begin{aligned} \hat{x}_k^+ &= E(x_0) \\ P_0^+ &= E[(x_0-\hat{x}_0^+)(x_0-\hat{x}_0^+)^T] \end{aligned} \tag{11}$$

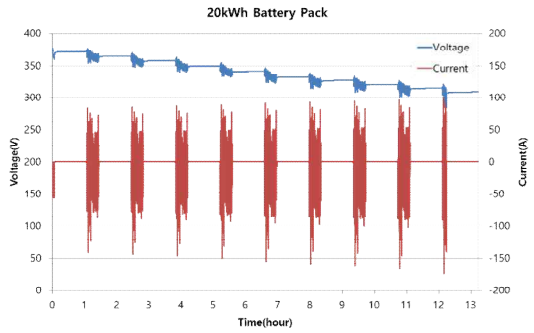


(a) Voltage and current of battery pack

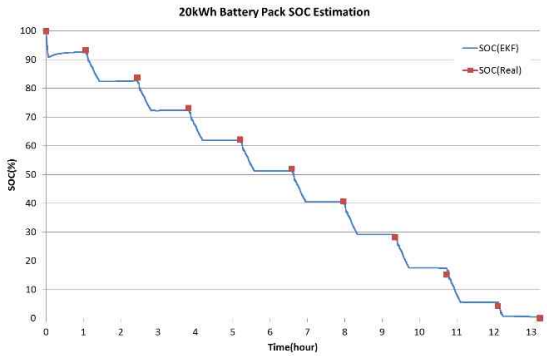


(b) SOC estimation according to reference SOC

**Fig. 10.** Result of SOC estimation using the EKF Method

**Table 5.** SOC error from estimation using the EKF Method

| No. | Measure Voltage | Estimation Voltage | SOC (Reference) | SOC (EKF) | Error (%) |
|---|---|---|---|---|---|
| 1 | 376.42 | 375.71 | 99.92 | 99.00 | -0.92 |
| 2 | 370.81 | 370.36 | 93.26 | 92.67 | -0.59 |
| 3 | 364.22 | 363.59 | 83.69 | 82.6 | -1.09 |
| 4 | 357.39 | 356.9 | 73.11 | 72.33 | -0.78 |
| 5 | 349.22 | 348.97 | 62.22 | 61.89 | -0.33 |
| 6 | 340.85 | 340.3 | 52.05 | 51.36 | -0.69 |
| 7 | 332.14 | 331.99 | 40.68 | 40.45 | -0.23 |
| 8 | 326.45 | 326.90 | 28.16 | 29.12 | +0.96 |
| 9 | 320.25 | 321.55 | 15.15 | 17.47 | +2.32 |
| 10 | 314.09 | 314.84 | 4.29 | 5.56 | +1.27 |
| 11 | 308.08 | 311.82 | 0 | 0.47 | +0.47 |

2) $k$-value operation: ($k$ = 1, 2, …)

State estimate time update: $\hat{x}_k^- = f(\hat{x}_{k-1}^+, u_{k-1})$

Error covariance calculation: $P_k^- = \hat{A}_{k-1} \cdot P_{k-1}^+ \cdot \hat{A}_{k-1}^T + S_w$

Kalman gain calculation: $L_k = P_k^- \hat{C}_k^T [\hat{C}_k \cdot P_k^- \cdot \hat{C}_k^T + S_v]^{-1}$

Estimation calculation: $\hat{x}_k^+ = \hat{x}_k^- + L_k[y_k - g(\hat{x}_k^-, u_k)]$

Error covariance calculation: $P_k^+ = (I - L_k \hat{C}_k) P_k^-$

### 3.2 Verification of SOC algorithm using EKF estimation method

The verification tests are conducted at various conditions to obtain the accuracy of the SOC estimation algorithm using the EKF. The verification tests show that the error between the voltage measured from the battery pack testing and the voltage estimated by the EKF is within 0.19–1.21% for the UDDS profile. Further, the estimated SOC and the measured SOC values were compared, and the error was 0.23% to 2.32%. The results obtained from the SOC verification test are shown in Fig. 10 and Table 5.

## 4. Conclusion

In this paper, the characteristics of the high-capacity lithium secondary battery are represented by mathematical differential equations and the parameters of the lithium secondary battery cells are extracted at various temperatures, ranging from high temperature to low temperature, through the battery modeling using the state space equation. A MATLAB tool was used to find the combination of the extracted parameters with minimum error. The extracted parameters were expressed as polynomial coefficients and optimized to be applied to various temperature ranges. The SOC is estimated using the optimized parameters represented by the state space equation. The estimated SOC is compared with the real SOC value acquired from the battery pack testing with a capacity of 20 kWh for the EV. The difference between the real SOC of the battery pack measured from the battery pack test and the estimated SOC using the EKF algorithm were within 2.3% and the feasibility of the study is confirmed. Through this study, the proposed SOC estimation method using the EKF shows a satisfactory accuracy and can be used as an SOC estimation method even in the dynamic situation of a 400-V high-voltage battery pack for the electric vehicle.

## Acknowledgement

This work was supported by the National Research Foundation of Korea(NRF) grant funded by the Korea government(MSIT) (No. NRF-2017R1C1B2010057)

## References

[1] D. H. Kim, M. J. Kim, and B. K. Lee, “An Integrated Battery Charger with High Power Density and Efficiency for Electric Vehicles,” *IEEE Trans. Power Electr.*, vol. 32, no. 6, pp. 4553-4565, June 2017.

[2] A. Emadi, Y. J. Lee, K. Rajashekara, “Power electronics and motor drives in electric, hybrid electric, and plug-in hybrid electric vehicles” *IEEE Trans. Ind. Electron*., vol. 55, no. 6, pp. 2237-2245, Jun. 2008.

[3] Y. Xing, W. He, M. Pecht, K. L. Tsui, “State of charge estimation of lithium-ion batteries using the open-circuit voltage at various ambient temperatures,” *Applied Energy*, vol. 113, pp. 106-115, Jan. 2014.

[4] J. Yi, U. S. Kim, C. B. Shin, T. Han, S. Park, “Modeling the temperature dependence of the discharge

behavior of a lithium-ion battery in low environmental temperature," *Journal of Power Sources*, vol. 244, pp. 143-148, Dec. 2013.
[5] C. Hu, B. D. Youn, J. Chung "A multiscale framework with extended Kalman filter for lithium-ion battery SOC and capacity estimation," *Applied Energy*, vol. 92, pp. 694-704, Apr. 2012.
[6] Plett, G., "Extended Kalman Filtering for Battery Management Systems of LiPB-Based HEV Battery Packs−Part 1: Background," *Journal of Power Sources*, vol. 134, no. 2, pp. 252-261, Aug. 2004.
[7] Plett, G., "Extended Kalman Filtering for Battery Management Systems of LiPB-Based HEV Battery Packs−Part 2: Modeling and Identification," *Journal of Power Sources*, vol. 134, no. 2, pp. 262-276, Aug. 2004.
[8] Plett, G., "Extended Kalman Filtering for Battery Management Systems of LiPB-Based HEV Battery Packs−Part 3: State and Parameter Estimation," *Journal of Power Sources*, vol. 134, no. 2, pp. 277-292, Aug. 2004.
[9] Plett, G., "Recursive approximate weighted total least squares estimation of battery cell total capacity," *Journal of Power Sources*, vol. 196, no. 4, pp. 2319-2331, Feb. 2011.

**Jinho Park** He received his B.S. degree in Mechanical Engineering from Hanyang University, Seoul, Korea in 1989 and his M.S. in Mechanical Engineering from University of Alabama, Tuscaloosa, Al, USA, in 1991. From 1992 to 1999, he worked for Mando Machinery Corporation as a research engineer. From 1999 to 2003, he worked for Bosch Electrical Drives Corporation as a senior research engineer. He is currently working toward the Ph. D. degree in Information & Communication Engineering at Sungkyunkwan University, Suwon, Korea. Since 2003, he has worked for Hyundai Motor Company in R & D Division as a General Manager. His research area is high voltage battery system application into the eco-friendly vehicles including HEV, PHEV, EV and FCEV.

**Byoung-Kuk Lee** He received the B.S. and the M.S. degrees from Hanyang University, Seoul, Korea, in 1994 and 1996, respectively and the Ph.D. degree from Texas A&M University, College Station, TX, USA, in 2001, all in electrical engineering. From 2003 to 2005, he was a Senior Researcher with Power Electronics Group, Korea Electrotechnology Research Institute, Changwon, Korea. From 2006, he is with the College of Information and Communication Engineering, Sungkyunkwan University, Suwon, Korea. His research interests include on-board charger and wireless power transfer for electric vehicles, energy storage systems, hybrid renewable energy systems, dc distribution systems for home appliances, power conditioning systems for fuel cells and photovoltaic, modeling and simulation, and power electronics. Prof. Lee received the Outstanding Scientists of the 21st Century from IBC and listed on 2008 Ed. of Who's Who in America and 2009 Ed. of Who's Who in the World. He is an Associate Editor in the IEEE Transactions On Industrial Electronics and Guest Associate Editor in the IEEE Transactions On Power Electronics. He was the Presenter for Professional Education Seminar with the topic of "On-Board Charger Technology for EVs and PHEVs" at the IEEE Applied Power Electronics Conference in 2014 and was the General Chair for the IEEE Vehicular Power and Propulsion Conference in 2012.

**Do-Yang Jung** He received the B.S. and the M.S. degrees from Hanyang University, Seoul, Korea, in 1988 and 1990, respectively and the Ph.D. degree from Ajou University. From 1993 to 1998, he worked for Daewoo Motors in the technical institute. From 1998 to 2001, he worked for Institute for Advanced Engineering. From 2001 to 2003, he worked for Nesscap Corporation. From 2003 to 2009 he worked for LG Chemistry in the institute of the battery research. From, 2009 to 2014 he was Vice-president of PNE solution. Since 2015, he has worked for PNE Systems Corporation a CEO. His research area is battery system application into the eco-friendly vehicles including HEV, PHEV, EV and FCEV.

**Dong-Hee Kim** He received the B.S., the M.S., and the Ph.D. degrees from Sungkyunkwan University, Suwon, Korea, in 2009, 2011, and 2015, respectively, all in electrical engineering. From 2015 to 2016, he was a postdoc researcher in Sunkyunkwan University. From 2016, he was a part-time lecturer in Daejin University, Korea and Shandong University of Technology, China, respectively. From Sep. 2016 to Aug. 2017, he was Assistant Professor in Tongmyong University, Busan, Korea. From Sep. 2017, he joined Chonnam National University, Gawangju, Korea, as an Assistant Professor. His research interests include power conditioning system dc-dc converters for renewable energy, and battery chargers for hybrid electric vehicles/electric vehicles.